Available online at www.sciencedirect.com
SCIENCE DIRECT®
Journal of Molecular and Cellular Cardiology 35 (2003) 795–802
Journal of Molecular and Cellular Cardiology
www.elsevier.com/locate/yjmcc

Original Article

Development of the coronary arteries in a murine model of transposition of great arteries

M. González-Iriarte [a], R. Carmona [a], J.M. Pérez-Pomares [a], D. Macías [a], M. Costell [b], R. Muñoz-Chápuli [a,*]

[a] *Department of Animal Biology, Faculty of Science, University of Málaga, Málaga 29071, Spain*
[b] *Department of Biochemistry and Molecular Biology, University of Valencia, Valencia, Spain*

Received 17 December 2002; received in revised form 24 February 2003; accepted 24 March 2003

Abstract

Transposition of great arteries in humans is associated with a wide spectrum of coronary artery patterns. However, no information is available about how this pattern diversity develops. We have studied the development of the coronary arteries in mouse embryos with a targeted mutation of perlecan, a mutation that leads to ventriculo-arterial discordance and complete transposition in about 70% of the embryos. The perlecan-deficient embryos bearing complete transposition showed a coronary artery pattern consisting of right and left coronary arteries arising from the morphologically dorsal and ventral sinuses of Valsalva, respectively. The left coronary artery gives rise to a large septal artery and runs along the ventral margin of the pulmonary root. In the earliest embryos where transposition could be confirmed (12.5 d post coitum), a dense subepicardial vascular plexus is located in this ventral margin. In wild-type mice, however, capillaries are very scarce on the ventral surface of the pulmonary root and the left coronary artery runs dorsally to this root. We suggest that the establishment of the diverse coronary artery patterns is determined by the anatomical arrangement and the capillary density of the peritruncal vascular plexus, a plexus that spreads from the atrio-ventricular groove and grows around the aortic or pulmonary roots depending on the degree of the short-axis aortopulmonary rotation. This simple model, based on very few assumptions, might explain all the observed variation of the coronary artery patterns in humans with transposition, as well as our observations on the perlecan-deficient and the normal mice.

Keywords: Transposition of great arteries; Perlecan; Outflow tract; Coronary artery development

1. Introduction

Transposition of great arteries (TGA) with ventriculo-arterial discordance is a severe congenital malformation characterized by the aorta arising from the anatomically right ventricle and the pulmonary trunk emerging from the anatomically left ventricle [1]. TGA frequently involves a right and slightly anterior (ventral) position of the aortic root respect to the pulmonary trunk, as well as the absence of a fibrous mitro-aortic continuity [2]. This malformation, which keeps pulmonary and systemic circulation in parallel instead of in series, is lethal in newborns due to generalized hypoxia unless venous and oxygenated blood can partially mix through atrial and/or ventricular septal defects. Even in this case the malformation is life threatening and requires urgent surgical intervention, which usually involves an arterial switch with coronary artery translocation. However, unusual coronary artery patterns are frequently found in TGA. For that reason, knowledge of coronary artery anatomy in TGA is of critical importance for the surgeon.

There are abundant data in the literature about the extensive variability of coronary artery patterns associated with TGA [2–4]. However, no information is hitherto available about how such a diverse spectrum of anatomical patterns develops. The study of the genesis of the coronary patterns associated with TGA is complex due to two factors: (1) the lack of good animal models for this pathology and (2) the occurrence of two independent but concomitant events in coronary morphogenesis, i.e. the assembly of a subepicardial capillary network [5–10] and the process of outflow tract septation coupled to the morphogenesis of the aortic and pulmonary valves [11–17]. These two developmental events meet when the aortic root is finally penetrated by the per-

* Corresponding author. Tel.: +34-952131853; fax: +34-952131668.
E-mail address: chapuli@uma.es (R. Muñoz-Chápuli).

DOI: 10.1016/S0022-2828(03)00134-2

itruncal portion of the subepicardial capillary plexus [18,19], a process starting around 13 d post coitum (dpc) in mouse embryos and that is completed around 13.5–14 dpc [20]. The mechanisms that determine the point of penetration of the peritruncal plexus into the aortic wall and the reasons why the pulmonary trunk is excluded from such penetrations are unknown [21, 22].

We have reported a high incidence of malformations in the OFT of mouse embryos with a targeted mutation of perlecan, frequently leading to complete TGA [23]. Perlecan is a heparan sulfate proteoglycan abundantly expressed in pericellular matrices and basement membranes during development [24]. Perlecan-null mice constitute the animal model of complete TGA which displays features more similar to the human pathology.

We aim, in this paper, to describe the coronary artery pattern in our model of TGA as well as to follow the genesis of this pattern associated with the development of the malformation. We think that the results obtained can provide interesting information to explain basic aspects of the establishment of the normal coronary artery pattern in mammals, including humans.

2. Materials and methods

Perlecan-deficient mice were generated by gene targeting, as previously described [25]. Genotyping of the embryos was performed by Southern blot analysis of EcoRI-digested genomic DNA obtained from tail fragments. Twelve homozygous, perlecan-null embryos were studied, at the stages 12.5 (3), 13.5 (2), 14.5 (4), 15.5 (2) and 17.5 dpc (1). Control embryos were five littermates at the stages 12.5 (2+/+), 14.5 (1+/–), 15.5 (1+/–) and 17.5 dpc (1+/–). Four additional wild-type control embryos of 12.5 and 13 dpc were included in order to study the anatomical arrangement of the peritruncal plexus.

For histology and immunohistochemistry, the embryos were fixed in 4% buffered paraformaldehyde in PBS or in methanol/acetone/water (2:2:1), dehydrated and paraffin embedded. Ten-micrometer sections were stained with hematoxylin– eosin or immunostained. Three wild-type control embryos (12.5 dpc) were fixed by cryosubstitution. Briefly, they were snap frozen in a cryotube placed in dry ice cooled with liquid nitrogen. Then, they were placed in methanol precooled in the same liquid nitrogen–dry ice mixture. Frozen embryos were kept in methanol at –80 °C for 5 d. Then, the embryos in methanol were kept at –20 °C for 6 h, washed twice with methanol at 4 °C (45 min) and twice with methanol at room temperature. Dehydration was completed in methanol/butanol (1:1) (20 min) and pure butanol (20 min). Then the embryos were paraffin embedded.

For immunoperoxidase staining, endogenous peroxidase and endogenous biotin were blocked and non-specific binding sites were saturated with 16% sheep serum, 1% bovine serum albumin and 0.5% Triton X-100 in Tris–PBS (SBT). The slides were then incubated overnight in mouse anti-

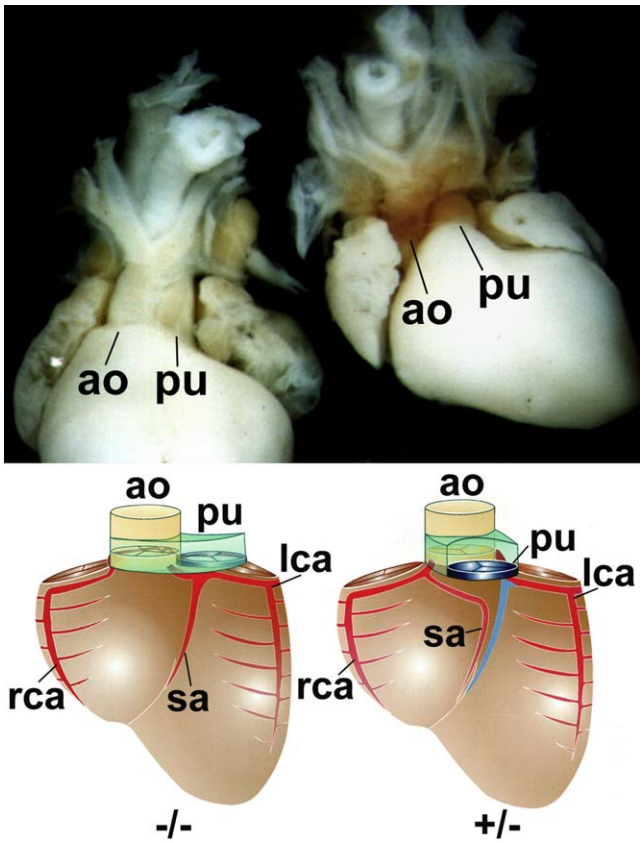

Fig. 1. Cardiac phenotype of the perlecan-deficient mouse embryos. (Top) Hearts of two 17.5 dpc embryos, an homozygous mutant (left) and a wild-type littermate (right). Differences in the anatomical arrangement of the great arteries are evident. The side-by-side arrangement of the aorta (AO) and pulmonary trunk (PU) is clearly visible in the mutant embryo. The littermate shows a normal condition, with the aorta arising behind the pulmonary trunk. (Bottom) Scheme of the anatomical arrangement of the main coronary arteries in mouse embryos bearing transposition (left) and wild-type control (right). Note the dorsal connection of the RCA to the aortic root, and the small branch, which arises from the RCA and runs dorsally to the pulmonary trunk. The septal artery (SA) arises from the LCA, in mice bearing transposition, or from the RCA in normal mice, although a case of SA arising from the LCA was observed (in blue). Partly reproduced from Costell et al. [23] with the permission of Lippincott, Williams and Wilkins.

smooth muscle cell (SMC) α-actin (clone 1A4, Sigma) diluted 1:2000 in SBT or in the endothelial marker rat anti-PECAM (clone Mec13.3, Pharmingen) diluted 1:10. Then, the slides were washed, incubated for 1 h in biotin-conjugated secondary antibody diluted 1:100 in SBT, washed again and incubated for 1 h in avidin–peroxidase complex diluted 1:150 in Tris–PBS. Peroxidase activity was developed with Sigma Fast® DAB tablets.

3. Results

3.1. Coronary artery pattern in mice displaying TGA (14.5–17.5 dpc)

The coronary artery pattern was studied in late embryos, since the mutation is lethal for newborns.

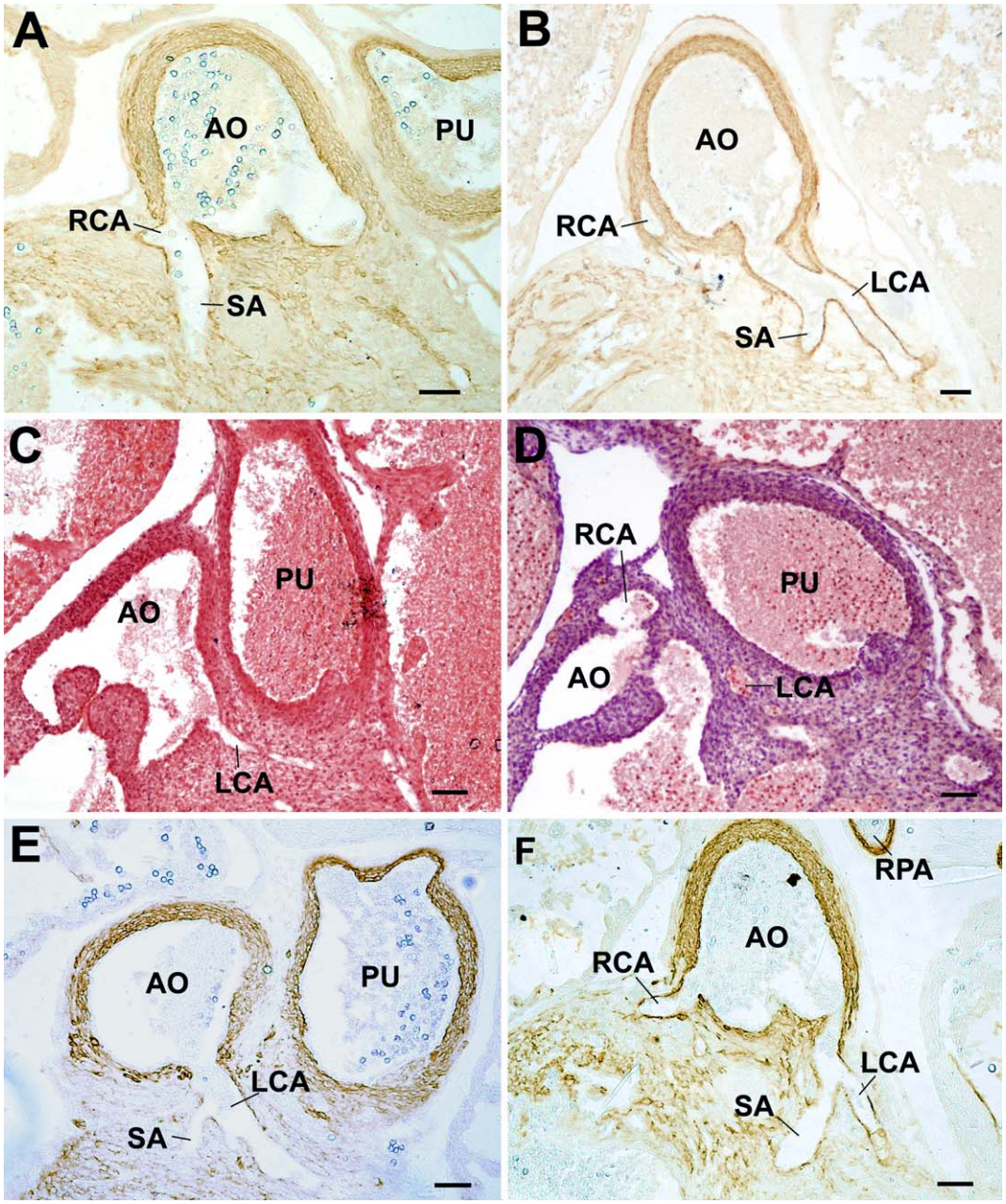

Fig. 2. Anatomical arrangement of the coronary arteries in perlecan-deficient and in control mouse embryos. Sections A, B, E and F are immunostained with antibodies against SMC specific α-actin. Sections C and D are hematoxylin–eosin stained. (A,B) Control embryos (heterozygous littermates), 14.5 and 15.5 dpc, respectively. It is shown the origin of the RCA and the LCA from the aorta (AO). The normal origin of the septal artery (SA) from the RCA is shown in (A). An anomalous origin of an SA from the LCA is shown in (B). PU: pulmonary trunk. Scale bar: 50 μm. (C,D) Perlecan-deficient embryos bearing TGA, 14.5 and 15.5 dpc, respectively. The origins of the RCA and the LCA are, respectively, shown in these figures. RCA arises from the morphologically dorsal sinus of Valsalva, while LCA runs along the ventral margin of the PU. Scale bar: 50 μm. (E) Perlecan-deficient embryo bearing TGA associated with an interventricular septal defect, 14.5 dpc. The septal branch arises from the LCA, but it is much reduced. Scale bar: 50 μm. (F) Perlecan-deficient embryo without TGA, but with a dextroposed AO, 14.5 dpc. The SA arises from the LCA, but the origin of both main coronary arteries is normal. RPA: right pulmonary artery. Scale bar: 50 μm.

Control embryos, in stages between 14.5 and 17.5 dpc, showed aortic and pulmonary trunks normally arranged, with the aortic root located dorsally to the pulmonary one (Fig. 1). The coronary artery pattern was constituted of intramyocardial arteries. The left coronary artery (LCA) and the right coronary artery (RCA) arise from the morphologically left and right Valsalva's sinuses, respectively (Figs. 1 and 2A,B) and supply the free walls of the corresponding ventricles. A septal artery usually arises from the RCA and branches to supply the interventricular septum (Fig. 2A). However, one of the three heterozygous embryos showed a main septal branch arising from the LCA (Fig. 2B), although a smaller branch was also observed arising from the RCA and supplying the interventricular septum.

Perlecan-null mouse embryos showed aortic and pulmonary roots arranged side by side, with the aortic root usually

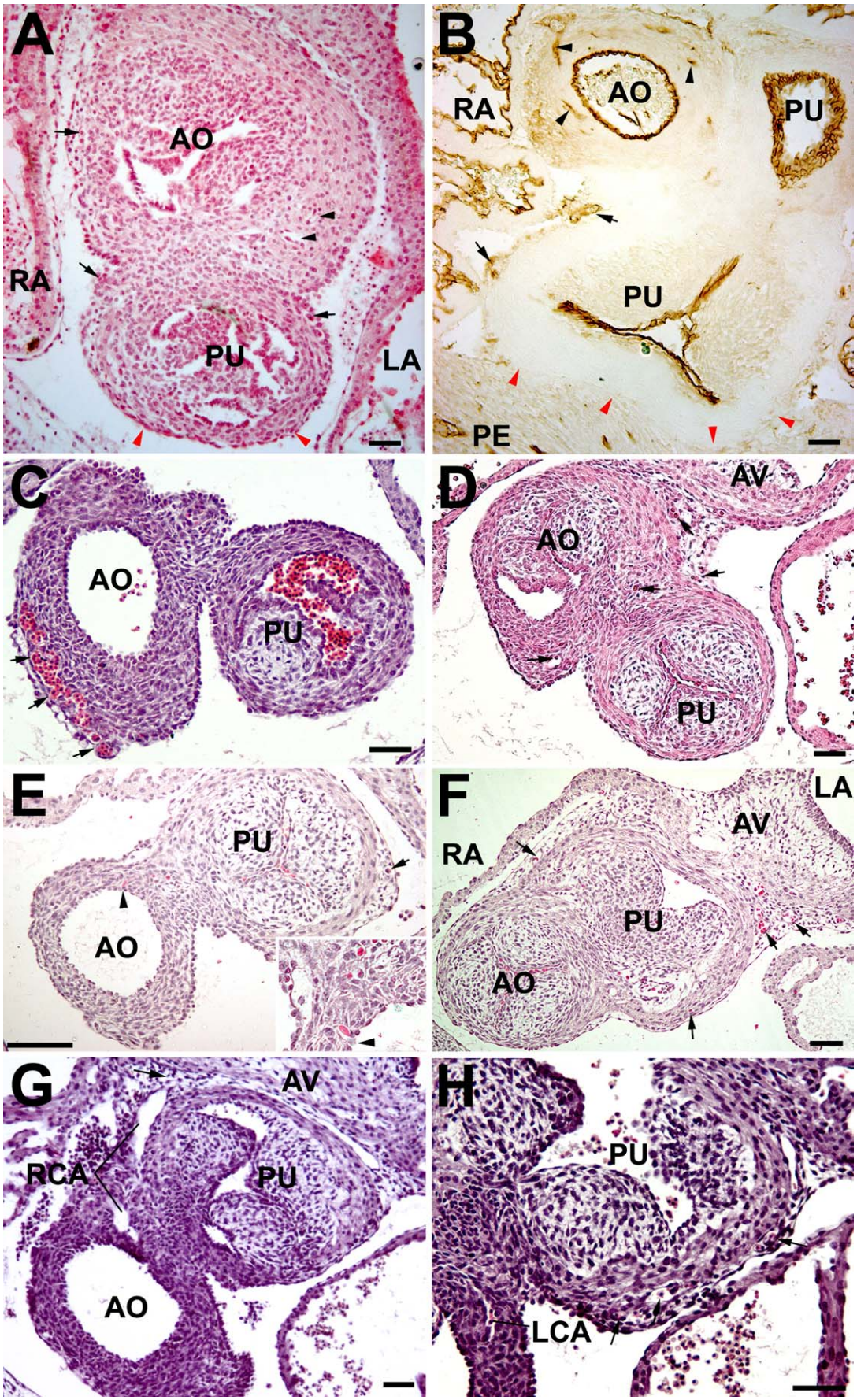
A
AO
RA
PU
LA
B
RA
AO
PU
PU
PE
C
AO
PU
D
AV
AO
PU
E
PU
AO
F
LA
AV
RA
PU
AO
G
AV
RCA
PU
AO
H
PU
LCA

located at a slightly more ventral level (Fig. 1). Ventricular septation was complete in the perlecan-deficient embryos studied except for one embryo, which showed a wide interventricular septal defect. One perlecan-deficient embryo (14.5 dpc) showed ventriculo-arterial concordance, although the aortic root was dextropositioned when compared with the normal embryos.

The perlecan-deficient mouse embryos displaying complete TGA showed a constant coronary artery pattern. This pattern consisted of an RCA arising from the morphologically dorsal sinus of Valsalva (which corresponds to the normal left sinus or sinus 2 from the Leiden convention [26]) and an LCA, which arises from the morphologically ventral sinus of Valsalva (which corresponds to the normal right sinus or sinus 1 from the Leiden convention) (Figs. 1 and 2C,D). The RCA gives rise to a small branch which runs towards the left, passing dorsally to the pulmonary trunk, and then it turns to the right, first and towards the apex cordis later, supplying the free wall of the right ventricle. The LCA soon gives rise to a large septal artery, which branches and supplies the interventricular septum. Then, the LCA runs along the ventral margin of the pulmonary root and branches to supply the free wall of the left ventricle (Fig. 2C). The embryo with a ventricular septal defect showed a narrow septal artery (Fig. 2E).

In the only perlecan-deficient embryo which showed a ventriculo-arterial concordance, the artery pattern is identical to that above described for the control embryos, although with a septal artery arising from the LCA (Fig. 2F).

3.2. Development of the coronary arteries in mice displaying TGA (12.5–13.5 dpc)

Coronary artery development was studied in embryos from stages 12.5 to 13.5 dpc.

In control embryos the aortic root was in contact with the atrio-ventricular (AV) canal, and a subepicardial plexus of capillaries surrounds the base of the aorta (Fig. 3A). This capillary plexus also spreads over the lateral margins of the aorticopulmonary septum and covers its distal limit, where the aorta and the pulmonary trunk become separated. However, capillaries were scarce or absent on the ventral surface of the pulmonary trunk, where the subepicardial space is virtually lacking (Fig. 3A). The scarcity of capillaries on the non-facing surface of the pulmonary root, as well as the presence of intramural capillaries within the aortic wall, was confirmed by PECAM immunostaining (Fig. 3B).

Perlecan-null mouse embryos, in these stages, showed either TGA (Fig. 3E–H) or, only in one case, ventriculo-arterial concordance with dextroposition of the aorta (Fig. 3C,D). In the embryos where TGA could be confirmed, the pulmonary root was in contact with the AV canal, and a subepicardial vascular plexus was clearly visible in the base of the outflow tract (conoventricular groove). This plexus was continuous with the vascular plexus of the AV groove (Fig. 3F). A dense network of subepicardial vessels spreads on the ventral surface of the pulmonary root (Fig. 3E–H) and over the lateral margins of the aorticopulmonary septum and the adjacent wall of the aorta (Fig. 3E,F). The non-facing aortic wall, opposed to the pulmonary trunk, showed only a few capillaries on its surface. Capillaries perforating the aortic wall could be identified in some cases (insert in Fig. 3E). These capillaries were always located in the lateral areas of the aortic wall facing the pulmonary trunk, i.e. in the prospective pulmonary-facing sinuses of Valsalva (Fig. 3E).

In a perlecan-deficient embryo of 12.5 dpc, we observed a ventriculo-arterial concordance with the aortic root located at the right of the pulmonary trunk (Fig. 3C). However, the aortic root was in contact with the AV canal (Fig. 3D), and the capillary plexus did not surround the pulmonary trunk. Instead, large capillaries were observed on the aortic root (Fig. 3C).

In all the embryos studied from these stages, either perlecan-deficient or control, capillary plexuses were always found around the AV groove, and along the ventricular margins and the interventricular groove.

4. Discussion

The coronary arteries were considered for a long time as mere outgrowths of the aortic root [20,27–29]. This view was

Fig. 3. Anatomical arrangement of the peritruncal capillary plexus in perlecan-deficient and in control mouse embryos. Transverse sections. Hematoxylin–eosin staining except for B. (A) Control embryo, 13 dpc. The aorta (AO) is located dorsally to the pulmonary trunk (PU). Subepicardial capillaries can be seen around the aortic root and over the facing side of the PU (arrows). Other capillaries are located within the aortic wall (black arrowheads), but they are very scarce on the ventral side of the PU, where the subepicardial space is virtually lacking (red arrowheads). LA: left atrium; RA: right atrium. Scale bar: 40 μm. (B) Control embryo, 12.5 dpc. Immunostaining with antibodies against the endothelial marker PECAM-1. Capillaries are abundant around the aortic root (arrows) and within the aortic wall (black arrowheads). The PU wall is devoid of capillaries, which are very scarce or absent in the ventral margin of this artery (red arrowheads). PE: pericardium. Scale bar: 40 μm. (C,D) Perlecan-deficient embryo without TGA, but with a dextroposed aorta, 12.5 dpc. The AO is in contact with the AV groove, and the peritruncal capillaries are continuous with the capillaries located in the AV subepicardium (arrows in D). Note the presence of large capillaries on the aortic wall (arrows in C) but not on the PU. Scale bars: 50 μm. (E,F) Perlecan-deficient embryo bearing TGA, 12.5 dpc. Note the ventral position of the aorta in relation to the PU and the lack of a subepicardial space on the non-facing surface of the aortic wall. The PU is in contact with the AV groove, and its root is completely surrounded by a wide subepicardial space containing capillaries (arrows), although these capillaries do not penetrate into the pulmonary wall. Instead, they can be seen within the pulmonary-facing aortic wall, opening even into the aortic lumen (arrowhead and insert in E). Scale bars: 50 μm. (G,H) Perlecan-deficient embryo bearing TGA, 13.5 dpc. The PU is surrounded by capillaries (arrows in H), but the main coronary arteries (RCA and LCA) are already visible within the aortic wall. Note the course of the RCA towards the area of high density of capillaries in the AV groove (arrow in G). Scale bars: 50 μm.

challenged in the late 1980s by the pioneering work of the Leiden group [18]. As already indicated, descriptive and experimental findings showed that coronary endothelial precursors self-organized in the subepicardial space forming a vascular plexus, which only in later stages connects to the aorta. Despite all these new insights in coronary morphogenesis, a pivotal question still remains unanswered: how the connections between the vascular plexus and the aorta are determined? The frequency of anomalous connections between the coronary arteries and the non-coronary aortic sinus or the pulmonary sinuses is relatively low. Only a 0.7% of the adult human population shows coronary artery anomalies, including anomalous origin or course of these arteries [30,31]. It suggests that a mechanism of unknown nature precisely controls the sites where the peritruncal capillaries perforate the aortic wall to open into the lumen of the Valsalva sinuses. It has been suggested that the neural crest can play some role in this determination, since the ablation of the cardiac neural crest generates anomalies in the aorta-coronary arteries connection [32]. Later studies, however, indicate that neural crest cells are essential for the persistence rather than for the formation of vessels [33]. This might indicate that neural crest cells are necessary to stabilize the media of the arteries but do not necessarily determine the place where the endothelial beds develop nor guide their spatial patterning. Among the alternative mechanisms to explain the penetration of the capillaries into the aortic root could be considered the asymmetric expression of genes between the aortic and the pulmonary trunks [34], mechanisms controlling differential apoptosis in the root of the outflow tract [21,35,36], and localization of the parasympathetic cardiac ganglia [32].

The perlecan-deficient model of TGA provides us not only a valuable system to study the mechanisms involved in this severe congenital malformation but possibly also a model to study the genesis of anomalous patterns of coronary artery anatomy. We are here in relating these anomalous patterns with the malposition of the aorta and the pulmonary trunk; although given the established role of perlecan in angiogenesis, we cannot rule out a direct role of this molecule in anomalies of the coronary artery development. We should also be cautious on this point because of the different arrangement of the coronary arteries in mice and humans; main coronary arteries are subepicardial in the latter and intramyocardial in the former. Nevertheless, the similarities between the normal anatomical pattern of the coronary arteries of mice and human seem to be significant. In both cases an LCA and an RCA arise from the left and right Valsalva sinuses, respectively, to supply the corresponding free walls of the ventricles. In humans, an anterior descending branch arises from the LCA and runs along the anterior interventricular groove giving rise to perforating branches towards the interventricular septum. This anterior descending artery, so often involved in acute cases of myocardial infarction after its occlusion, is functionally replaced in mice by an intramyocardial septal artery branch that supplies the interventricular septum. The existence of this septal branch is a characteristic feature of all the micromammals studied hitherto [37]. However, the origin of the septal artery is variable. In wild mice, as well as in laboratory strains, it normally arises from the RCA [37,38]. In one of the control embryos studied by us, a heterozygous littermate of the perlecan-deficient mice, we have found a main septal branch arising from the LCA, with a smaller branch sprouting from the RCA. We think that this can be rather explained in terms of the normal variability of the origin of this branch than by the heterozygous condition of this embryo.

Perlecan-deficient mice displaying TGA showed a constant coronary artery pattern consisting of an RCA arising from the morphologically dorsal aortic sinus (corresponding to the left sinus in a non-transposed arrangement) and an LCA, which arises from the morphologically ventral sinus (i.e. the right sinus from a normal heart). This LCA gives rise to the septal artery and runs along the ventral margin of the pulmonary root to branch in the free wall of the left ventricle (Fig. 4).

Assuming that the septal artery of mice corresponds functionally to the anterior descending artery of human, the coronary pattern found in the perlecan mice agrees with type I from the classification of Shaher [39]. This is the most frequent variant found in human TGA, since it appears in about 70% of the cases [4]. This reinforces our proposal that TGA in perlecan-deficient mice is very similar to the human malformation.

A whole account about the coronary artery pattern in TGA has proposed a modification of the original Shaher's classification establishing a relationship between the coronary artery pattern and the degree of the short-axis aortopulmonary rotation [2]. These authors showed an increase in the frequency of the Shaher's types 0, I, II, IV and IX as the aorta was located in positions (relative to the pulmonary trunk) left anterior, anterior, right anterior, right or right posterior, respectively (Fig. 4). The TGA found in perlecan-null mice consistently shows an aorta located right ventral (i.e. anterior) to the pulmonary trunk, an anatomical arrangement what corresponds, in humans, to a higher frequency of the coronary pattern types I and II [2]. As we have said above, perlecan-null mice consistently showed a Shaher's pattern type I. However, it is interesting to note the presence of a small branch arising from the RCA and running dorsally to the pulmonary trunk. This would allow us to consider also the coronary pattern of the perlecan-deficient mice within the Shaher's type VIII, a subtype of the pattern II characterized by two arteries irrigating the left ventricle and running dorsal and ventral to the pulmonary trunk. Thus, the coronary pattern found in perlecan-deficient mice bearing TGA agrees well with the prediction made according to the right ventral position of the aorta.

The relation of the orientation of the aorticopulmonary axis with the development of a precise coronary artery pattern lead us to consider the developmental stages previous and immediately posterior to the connection between the

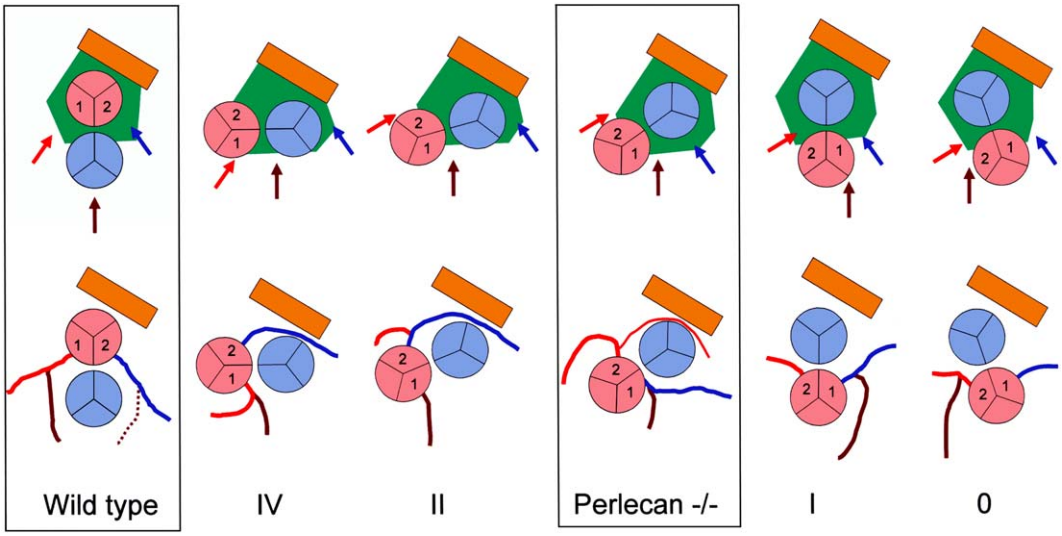

Fig. 4. Model on the relationship between the development of the peritruncal capillary plexus and the anatomical arrangement of the main coronary arteries in TGA. Aortic and pulmonary trunks are represented in pink and blue, respectively. The region of the AV canal is represented by an orange rectangle. Right, left and septal coronary arteries are depicted in red, blue and brown colour, respectively. The coronary Valsalva sinuses are labeled as 1 and 2 according to the Leiden convention [26]. In the bottom row, the anatomical arrangement of the coronary arteries found in wild-type and perlecan-deficient mice is shown in relation with some of the coronary patterns described in humans with TGA [2]. In the top, it is shown (in green) the area where the peritruncal capillary plexus was observed in wild-type and perlecan-deficient mice bearing TGA, as well as the most probable ways of connection of the peritruncal plexus with the capillary plexuses, which are developing into the right and left ventricles and the interventricular septum (red, blue and brown arrows, respectively). We suggest that the hypothetical distribution of peritruncal capillaries shown for the coronary pattern types 0–IV can explain their development, assuming that the main coronary arteries develop in the areas of higher capillary density (in green) and that the pulmonary trunk is forbidden for capillary penetration. In this way, the course of the LCA dorsal or ventral to the pulmonary trunk (patterns IV–II vs. patterns I–0) would depend on the presence of capillaries ventral to this trunk. On the other hand, the connection of the septal artery to the LCA, the RCA or directly to the Valsalva sinus 1, would depend on the location of the closest areas of the peritruncal plexus to the capillaries which are developing into the interventricular septum.

peritruncal capillary plexus and the aortic lumen, i.e. at the stages 12.5–13.5 dpc. In these stages, we have described significant differences in the distribution and density of the truncal capillary plexus between the perlecan-deficient mice, which are developing TGA, and the control littermates or even the mutant embryos in which TGA is not achieved. Thus, in mutant embryos bearing TGA, the pulmonary root is in contact with the AV canal, and a dense plexus of capillaries can be seen all around the proximal part of the pulmonary trunk. This plexus is in contact with the developing vessels of the AV groove and also in contact with other capillaries located between the aortic and pulmonary roots. However, in control embryos or in the mutant embryo with ventriculo-arterial concordance, this dense capillary network surrounds the aortic root, which is closer to the AV canal. Since the vessels constitutive of these networks are the basic elements in the differentiation of the main coronary branches, we think that there should be a close relationship between the anatomical arrangement of the subepicardial capillary networks and the final pattern of coronary arteries.

By combining this consideration with the proposal about the relation between the orientation of the aorticopulmonary axis and the coronary artery pattern [2], we suggest a model about the establishment of the anatomical arrangements of the coronary arteries in TGA. This model is based on embryological considerations and rests on two assumptions: (1) the wall of the pulmonary trunk is forbidden for the penetration of the capillaries of the plexus and (2) the arrangement of the main branches of the arterial coronary system is determined by the density of capillaries in the peritruncal plexus, a factor which depends of the local availability of vascular progenitors in the subepicardium. This model is depicted in Fig. 4, where we show our observations on the normal and mutant perlecan-deficient mice in relation to some coronary patterns described in humans bearing TGA, and we are making a prediction about the arrangement of the peritruncal capillary plexus which could explain the observed patterns in humans. As shown in Fig. 4, the course of the LCA dorsal or ventral to the pulmonary trunk (patterns IV–II vs. patterns I–0) would depend on the abundance of capillaries around this artery. On the other hand, the connection of the septal artery to the LCA or the RCA would depend on the location of the closest areas of the peritruncal plexus to the capillaries which are developing in the interventricular septum. As shown in Fig. 4, this connection will jump between the RCA and the LCA depending of the position of the “forbidden” peripulmonary areas relative to the network of capillaries which are developing into the interventricular groove.

We think that this simple model, based on very few assumptions, explains all the observed variation of the coronary artery patterns in TGA, as well as the normal pattern and our observations on the perlecan-deficient mice. However, as we have stated above, we cannot yet speculate about the mechanisms which preclude the penetration of capillaries in the pulmonary wall.

Acknowledgements

This work was supported by grants PM99-0179 and SAF2002-02651 (MCYT, Spain). We thank E. Pérez-Pomares and Dr. E. Manjón-Cabeza for their help designing the illustrative cartoons and Amalia Capilla and Mónica Gomez-Lor for genotyping mice and embryos.

References

[1] Thiene G, Frescura C. Cardiopatie congenite. In: Cali A, Fiore Donati L, editors. Anatomia patologica generale e applicata. Firenze: Uses; 1988. p. 795–837.
[2] Chiu IS, Chu SH, Wang JK, Wu MH, Chen MR, Cheng CF, et al. Evolution of coronary artery pattern according to short axis aortopulmonary rotation: a new categorization for complete transposition of the great arteries. J Am Coll Cardiol 1995;26:250–8.
[3] Angelini P, de la Cruz MV, Valencia AM, Sanchez Gomez C, Kearney DL, Sadowinski S, et al. Coronary arteries in transposition of the great arteries. Am J Cardiol 1994;74:1037–41.
[4] Sim EKW, van Son JAM, Edwards WD, Julsrud PR, Puga FJ. Coronary artery anatomy and complete transposition of the great arteries. Ann Thorac Surg 1994;57:890–4.
[5] Hiruma T, Hirakow R. Epicardial formation in embryonic chick heart: computer aided reconstruction, scanning and transmission electron microscopic studies. Am J Anat 1989;184:129–38.
[6] Mikawa T, Fischman DA. Retroviral analysis of cardiac morphogenesis: discontinuous formation of coronary vessels. Proc Natl Acad Sci USA 1992;89:9504–8.
[7] Poelmann RE, Gittenberger de Groot AC, Mentink MMT, Bökenkamp R, Hogers B. Development of the cardiac coronary vascular endothelium, studied with antiendothelial antibodies, in chicken quail-chimeras. Circ Res 1993;73:559–68.
[8] Viragh S, Gittenberger de Groot AC, Poelmann RE, Kalman F. Early development of quail heart epicardium and associated vascular and glandular structures. Anat Embryol 1993;188:381–93.
[9] Pérez-Pomares JM, Macías D, García Garrido L, Muñoz-Chápuli R. Contribution of the primitive epicardium to the subepicardial mesenchyme in hamster and chick embryos. Dev Dyn 1997;210:96–105.
[10] Pérez-Pomares JM, Macías D, García-Garrido L, Muñoz-Chápuli R. Immunolocalization of the vascular endothelial growth factor receptor 2 in the subepicardial mesenchyme of hamster embryos: identification of the coronary vessel precursors. Histochem J 1998;30:627–34.
[11] Hurle JM, Colvee E, Blanco AM. Development of mouse semilunar valves. Anat Embryol 1980;160:83–91.
[12] Kirby ML, Gale TF, Stewart DE. Neural crest cells contribute to normal aorticopulmonary septation. Science 1983;220:1059–61.
[13] Bockman DE, Redmond ME, Waldo K, Davis H, Kirby ML. Effect of neural crest ablation on development of the heart and arch arteries in the chick. Am J Anat 1987;180:332–41.
[14] Garcia-Martinez V, Sanchez-Quintana D, Hurle JM. Histogenesis of the semilunar valves: an immunohistochemical analysis of tenascin and type I collagen distribution in developing chick heart valves. Cell Tissue Res 1990;259:299–304.
[15] Ya J, van den Hoff MJ, de Boer PA, Tesink Taekema S, Franco D, Moorman AF, et al. Normal development of the OFT in the rat. Circ Res 1998;82:464–72.
[16] Van den Hoff MJ, Moorman AF, Ruijter JM, Lamers WH, Bennington RW, Markwald RR, et al. Myocardialization of the cardiac outflow tract. Dev Biol 1999;212:477–90.
[17] Qayyum SR, Webb S, Anderson RH, Verbeek FJ, Brown NA, Richardson MK. Septation and valvar formation in the outflow tract of the embryonic chick heart. Anat Rec 2001;264:273–83.
[18] Bogers AJJC, Gittenberger de Groot AC, Poelmann RE, Peault BM, Huysmans HA. Development of the coronary arteries, a matter of ingrowth or outgrowth? Anat Embryol 1989;180:437–41.
[19] Waldo KL, Willner W, Kirby ML. Origin of the proximal coronary artery stems and a review of ventricular vascularization in the chick embryo. Am J Anat 1990;188:109–20.
[20] Viragh S, Challice CE. The origin of the epicardium and the embryonic myocardial circulation in the mouse. Anat Rec 1981;201:157–68.
[21] Velkey JM, Bernanke DH. Apoptosis during coronary artery orifice development in the chick embryo. Anat Rec 2001;262:310–7.
[22] Bernanke DH, Velkey JM. Development of the coronary blood supply: changing concepts and current ideas. Anat Rec (New Anatomist) 2002;269:198–208.
[23] Costell M, Carmona R, Gustaffsson E, González Iriarte M, Fässler R, Muñoz Chápuli R. Hyperplastic conotruncal endocardial cushions and transposition of great arteries in perlecan null mice. Circ Res 2002;91:158–64.
[24] Handler M, Yurchenco PD, Iozzo RV. Developmental expression of perlecan during murine embryogenesis. Dev Dyn 1997;210:130–45.
[25] Costell M, Gustafsson E, Aszodi A, Mörgelin M, Bloch W, Hunziker E, et al. Perlecan maintains the integrity of cartilage and some basement membranes. J Cell Biol 1999;147:1109–22.
[26] Gittenberger de Groot AC, Sauer U, Oppenheimer-Dekker A, Quaegebeur J. Coronary arterial anatomy in transposition of the great arteries. A morphologic study. Pediatr Cardiol 1983;4:15–24.
[27] Grant RT. Development of the cardiac coronary vessels in the rabbit. Heart 1926;13:261–71.
[28] Dbaly J, Ostadal B, Rychter Z. Development of the coronary arteries in rat embryos. Acta Anat (Basel) 1968;71:209–22.
[29] Rychter Z, Ostadal B. Mechanism of the development of coronary arteries in chick embryo. Folia Morphol (Praha) 1971;19:113–24.
[30] Roberts WC. Major anomalies of coronary arterial origin seen in adulthood. Am Heart J 1986;111:941–63.
[31] Angelini P. Normal and anomalous coronary arteries: definitions and classification. Am Heart J 1989;117:418–34.
[32] Waldo KL, Kuminski DH, Kirby ML. Association of the cardiac neural crest with development of the coronary arteries in the chick embryo. Anat Rec 1994;239:315–31.
[33] Waldo KL, Kuminski DH, Kirby ML. Cardiac neural crest is essential for the persistence rather than the formation of an arch artery. Dev Dyn 1996;205:281–92.
[34] Chisaka O, Capecchi MR. Regionally restricted developmental defects resulting from targeted disruption of the mouse homeobox gene *hox 1.5*. Nature 1991;350:473–9.
[35] Watanabe M, Choudhry A, Berlan M, Singal A, Siwik E, Mohr S, et al. Developmental remodeling and shortening of the cardiac outflow tract involves myocyte programmed cell death. Development 1998;125:3809–20.
[36] Rothenberg F, Hitomi M, Fisher SA, Watanabe M. Initiation of apoptosis in the developing avian outflow tract myocardium. Dev Dyn 2002;223:469–82.
[37] Durán AC, Sans-Coma V, Arqué JM, Cardo M, Fernández B, Franco D. Blood supply to the interventricular septum of the heart in rodents with intramyocardial coronary arteries. Acta Zool 1992;73:223–9.
[38] Icardo JM, Colvee E. Origin and course of the coronary arteries in normal mice and in iv/iv mice. J Anat 2001;199:473–82.
[39] Shaher RM, Pudd GC. Coronary arterial anatomy in complete transposition of the great vessels. Am J Cardiol 1966;17:355–61.